Biochemical and Biophysical Research Communications 443 (2014) 911–916

Contents lists available at ScienceDirect

Biochemical and Biophysical Research Communications

journal homepage: www.elsevier.com/locate/ybbrc

Nucleotide-dependent displacement and dynamics of the α-1 helix in kinesin revealed by site-directed spin labeling EPR

Satoshi Yasuda [a], Takanori Yanagi [a], Masafumi D. Yamada [b], Shoji Ueki [c], Shinsaku Maruta [b], Akio Inoue [a], Toshiaki Arata [a,*]

[a] Department of Biological Sciences, Graduate School of Science, Osaka University, Toyonaka, Osaka 560-0043, Japan
[b] Division of Bioengineering, Graduate School of Engineering, Soka University, Hachioji, Tokyo 192-8577, Japan
[c] Kagawa School of Pharmaceutical Sciences, Tokushima Bunri University, Shido 1314-1, Samuki, Kagawa 769-2193, Japan

ARTICLE INFO

Article history:
Received 26 November 2013
Available online 19 December 2013

Keywords:
Kinesin-1
Neck-linker
Structural dynamics
Spin–spin distance
Electron paramagnetic resonance
Spin labeling
Dipolar EPR
Conventional kinesin
Molecular motor

ABSTRACT

In kinesin X-ray crystal structures, the N-terminal region of the α-1 helix is adjacent to the adenine ring of the bound nucleotide, while the C-terminal region of the helix is near the neck-linker (NL). Here, we monitor the displacement of the α-1 helix within a kinesin monomer bound to microtubules (MTs) in the presence or absence of nucleotides using site-directed spin labeling EPR. Kinesin was doubly spin-labeled at the α-1 and α-2 helices, and the resulting EPR spectrum showed dipolar broadening. The inter-helix distance distribution showed that 20% of the spins have a peak characteristic of 1.4–1.7 nm separation, which is similar to what is predicted from the X-ray crystal structure, albeit 80% were beyond the sensitivity limit (>2.5 nm) of the method. Upon MT binding, the fraction of kinesin exhibiting an inter-helix distance of 1.4–1.7 nm in the presence of AMPPNP (a non-hydrolysable ATP analog) and ADP was 20% and 25%, respectively. In the absence of nucleotide, this fraction increased to 40–50%. These nucleotide-induced changes in the fraction of kinesin undergoing displacement of the α-1 helix were found to be related to the fraction in which the NL undocked from the motor core. It is therefore suggested that a shift in the α-1 helix conformational equilibrium occurs upon nucleotide binding and release, and this shift controls NL docking onto the motor core.

1. Introduction

The motor protein kinesin moves along a microtubule (MT) using the chemical energy of ATP. In neurons, kinesin powers vesicular trafficking toward the synapse; in all cells, kinesin is involved in the restructuring that occurs during cell division [1–3]. All kinesins have a homologous ~330 amino acid catalytic core that binds ATP and microtubules (MTs). Immediately adjacent to the catalytic core is the neck linker (NL) – a ~15-amino acid segment that has been shown to be critical in force generation and directionality [4–8].

Site-directed spin labeling electron paramagnetic resonance (SDSL-EPR) spectroscopy has been used to determine the secondary, tertiary, and quaternary structures of proteins and to monitor associated conformational changes [9–11]. Depending on the mobility of the attached spin label, we can detect both the steric restrictions that are imposed on the label by its environment and the motion of a polypeptide chain segment [12,13]. Moreover, if two spin labels are close to each other, the resultant spectrum includes effects from dipole interactions and is dependent on the distance between the two spins [11]. We found that the transition of the NL from an undocked to a docked conformation occurred in the ATP-bound state but not in the ADP-bound state or no nucleotide state, suggesting that the NL is an ATP- and strain-dependent mechanical element [5–7,13,14]. Therefore, it is important to understand how nucleotides (ATP or ADP) bound in the active site can communicate with the NL to control NL docking on the kinesin core domain. These SDSL-EPR studies [15] suggest that two helices, switch I and switch II, undergo nucleotide-dependent conformational changes (analogous to conformational changes in G-proteins [16]) that play an important role in communicating between the catalytic site and the NL docking domain on the MT-binding interface of kinesin. Recent cryoelectron microscopy (cryo-EM) studies also revealed that these unique helices communicate between the catalytic site and the NL docking region [17–20].

Abbreviations: AMPPNP, adenosine 5′-(β,γ-imido)triphosphate; βME, 2-mercaptoethanol; CW, continuous wave; EGTA, ethylene glycol-bis(l-aminoethyl ether)-*N,N,N′,N′*-tetraacetic acid; EM, electron microscopy; MSL, 4-maleimido-2,2,6,6-tetramethyl-1-piperidinoxy; NN, no nucleotide; MT, microtubule; PIPES, piperazine-1,4-bis(2-ethanesulfonic acid); SDSL, site-directed spin labeling.

* Corresponding author. Fax: +81 6 6850 5441.
E-mail address: arata@bio.sci.osaka-u.ac.jp (T. Arata).

0006-291X/$ - see front matter © 2013 Elsevier Inc. All rights reserved.
http://dx.doi.org/10.1016/j.bbrc.2013.12.063

In kinesin X-ray crystal structures, the N-terminal region of the α-1 helix is adjacent to the adenine ring of the bound adenine nucleotide, while the C-terminal region of the helix is near the NL [21]. Here, we examine, using SDSL-EPR, the displacement of the α-1 helix relative to the α-2 helix of a kinesin monomer bound to MTs in the presence or absence of nucleotides. It is suggested that a shift in the equilibrium between two α-1 helix conformations occurs upon nucleotide binding and release and that this shift controls NL docking onto the motor core.

2. Materials and methods

Site-directed cysteine mutants of Cys-lite kinesin monomer (1–349 residues) were spin labeled by MSL [12–14] and their MT-activated ATPase activities were measured as described previously [22,23]. For the EPR measurements, the MT-bound kinesin (~50 μM) was incubated with either 2 mM adenosine 5′-(β,γ-imido)triphosphate (AMPPNP), 2 mM ADP, or 5 U/ml apyrase [12–14].

We estimated the effective rotational correlation time of spin label motion and the distance between spin labels from CW(continuous wave)-EPR measurements as described previously [13,14,24,25]. The dipolar spectra taken at 173 K were fit by changing 3 parameters: the center and full-width at half maximum of the distance distribution between the spin labels (modeled as single Gaussian) and the fraction of non-interacting spins. Experimental details were provided in the supplementary data.

3. Results and discussion

3.1. Functional properties of labeled kinesin mutants

We spin-labeled 7 kinesin mutants (V62C, S66C, A67C, M68C, I70C, K72C, R114C) with mutations in the α-1 and α-2 helices with MSL (Fig. 1). The labeling efficiency for kinesin, estimated from double integration of the spectrum, was >0.9 mol/mol cysteine residue.

We measured the MT-dependent ATPase activity of spin-labeled kinesin (Table 1). The MT-dependent ATPase activities (V_{max}) of the spin-labeled mutants were more than 50% of that of the WT Cys-lite kinesin. Furthermore, the ATPase activity in the presence of MTs was at least 600 times higher than basal ATPase activity. These results suggested that all the kinesin mutants retained near wild-type MT-dependent ATPase activity.

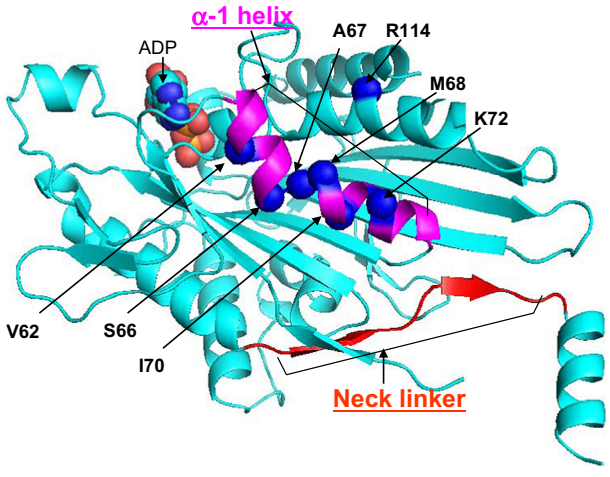

Fig. 1. Location of site-directed mutagenesis in the crystal structure of the kinesin motor domain (2KIN). The V62, S66, A67, M68, I70, K72 and R114 residues of mouse conventional kinesin monomer (1–349 residues) were mutated to cysteine and spin labeled. The mutated residues are represented by blue spheres. ADP is shown as a space-filling model. (For interpretation of the references to color in this figure legend, the reader is referred to the web version of this article.)

Table 1
Basal and MT-dependent V_{max} ATPase activity of spin-labeled kinesin mutants.

Sample	Basal ATPase (s^{-1})	V_{max} (s^{-1})[a]
Cys-lite[b]	0.013	27.5
V62C	0.022	13.9
S66C	0.030	17.9
A67C	0.027	16.5
M68C	0.010	19.3
I70C	0.011	18.9
K72C	0.010	25.1
R114C	0.020	24.6
K72C/R114C	0.012	18.0

[a] V_{max} was determined by measuring the ATPase rate in the presence of at least two saturating concentrations of MTs (10 μM and 20 μM).
[b] Not spin-labeled.

3.2. Nucleotide-dependent changes in the mobility of spin-labeled α-1 helix and α-2 helix side chains

We investigated the effect of bound MTs on the EPR spectra from monomeric kinesins mutated at the residues in the α-1 helix and α-2 helix in the ADP-bound state (Fig. 2A). The spectrum of the kinesin mutant spin-labeled at V62C on the α-1 helix in the ADP-bound state in the absence of MTs showed a mixture of fast (F) and slow (S) components. The effective rotational correlation time of the fast and slow components were nearly 1.50 ns and 19.4 ns, respectively. The peak height ratio of the fast to slow components was 1.13. Assuming that the height of the slow mobility peak represents approximately twice as many labels as the same height for fast mobility peak, then the fraction of the fast component was estimated to be 36%. These results indicated that the side chain of the V62C residue of the kinesin α-1 helix could have two conformations. When the spin-labeled V62C mutant was mixed with MTs, the EPR spectrum again showed a mixture of fast and slow components. However, the peak height ratio decreased to 0.50, and as a result, the fraction of fast components decreased to 20%. Other kinesin mutants showed the same tendency (Table 2). These results indicated that binding of MTs to the kinesin motor domain caused a conformational change in the α-1 and α-2 helix region, and these changes resulted in enhanced steric hindrance around these residues and/or reduced flexibility of the backbone of these helices.

We also examined the effect of nucleotide binding on spin label mobility in the α-1 helix side chains in the presence of MTs (Fig. 2B and C). In these experiments, the absorption line shapes of all mutants also had two components. The effective rotational correlation times of the fast and slow components, nearly 1.5 ns and 10–40 ns, respectively, were similar among all mutants in the presence of various nucleotides. The fraction of the fast component in the kinesin mutants labeled at V62C, S66C, A67C, M68C, I70C, K72C, and R114C with no nucleotide (NN) was 20%, 19%, 31%, 15%, 15%, 36%, and 14%, respectively (Table 2). For these mutants in the AMPPNP-bound state, the fraction of the fast component was estimated to be 22%, 21%, 31%, 19%, 17%, 40%, and 21%, respectively. For these residues in the ADP-bound state, the fraction of the fast component was estimated to be 20%, 20%, 29%, 24%, 17%, 39%, and 17%, respectively. Therefore, the fraction of the fast component in the NN state obtained from the M68C, K72C, and R114C mutants was larger than in the AMPPNP- or ADP-bound state. These results indicated that the binding of AMPPNP or ADP caused a conformational change of the α-1 and α-2 helix regions, eliminating steric hindrance around these residues.

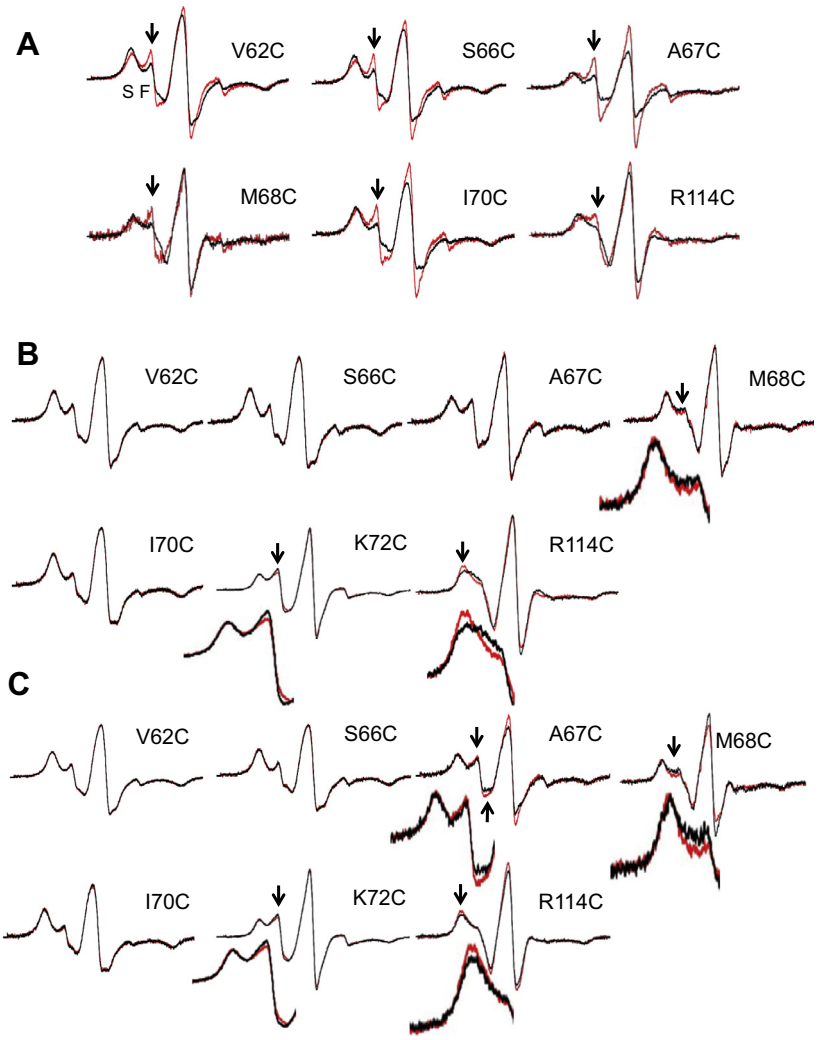

Fig. 2. Overlaid EPR spectra from spin labels attached to the V62C, S66C, A67C, M68C, I70C, K72C and R114C kinesin mutants. The spectra were taken at room temperature under several nucleotide conditions, both in the absence and presence of MT. (A) The ADP-bound state in the absence (red line) or presence (black line) of MT. (B) The AMPPNP-bound state (black line) and the apo or no nucleotide (NN) state (red line) in the presence of MT. (C) The ADP-bound state (black line) and the apo or NN state (red line) in the presence of MT. The scan width is 100 G. For V62C, the peaks from fast and slow components are indicated by F and S at lower magnetic field, respectively. The arrows show the peaks indicating significant spectral change. The insets show the magnified spectra at lower field, indicating significant change. (For interpretation of the references to color in this figure legend, the reader is referred to the web version of this article.)

3.3. Determination of interspin distances between M68C and R114C in the absence and presence of MTs

We measured dipolar interactions between two spin labels located at residues M68C and R114C using dipolar EPR spectroscopy to detect the conformational change of the kinesin α-1 helix induced by nucleotide-binding in the presence or absence of MTs. Fig. 3A shows the spectra of double-labeled kinesin monomer in the ADP-bound state in the absence of MTs at 173 K. A comparison of the double-labeled EPR spectrum for the MT-free kinesin with the spectrum of the single-labeled kinesin revealed clear spectral line broadening. The amplitude of the double-labeled spectrum appeared smaller (86%) than that of the single-labeled spectrum. This observation indicated that the spin–spin distances were less than 2.5 nm. Distance distributions were obtained using a spectral fitting method by assuming a single Gaussian distribution of distances and non-interacting spins (>2.5 nm) (Fig. 3A, left). The result showed a narrow Gaussian distribution centered at 1.40 nm with a full-width at half maximum of 0.07 nm (Fig. 3A, right). However, 79% of spins were beyond the sensitivity limit of the dipolar CW-EPR method (>2.5 nm), including a small amount of non-interacting spins (<10%) due to substoichiometric spin-labeling efficiency. The single Gaussian fits without assuming a population of >2.5 nm spins did not result in well-defined narrow distributions, as evidenced by the residual sum (χ^2) becoming 10–20% worse (data not shown). Fitting with two or three Gaussians did not result in a better fit (data not shown). These results demonstrated that the distribution of distances between the two spin labels attached at M68C and R114C has two different components. This result strongly suggested that the relative positions, at least the relative residual positions of the two helices, have two populations: one (21%) having a narrow inter-helix distance distribution centered at 1.4 nm and the remaining second population (79%) having an inter-helix distance beyond the 2.5-nm limit of detection. The narrow distance distribution (1.4 nm) is close to the 68Lys Nζ – 114His $N\varepsilon_2$ distance (1.49 nm), the 68Lys Cβ – 114His Cβ distance (1.14 nm), and the 68Lys Cα – 114His Cα distance (1.11 nm) from the crystal structure (2KIN) reported by Sack et al. [21]. However, the conformation with an inter-helix distance beyond sensitivity (>2.5 nm) is unexpected. (A more detailed distance distribution will be obtained using a pulsed EPR method in further studies. This technique is sensitive over longer distances of 2–8 nm [11,25].) Therefore, it is likely that either or both of the kinesin

Table 2
Summary of the effective rotational correlation time (τ) of the spin-labeled kinesin residues.

		τ (ns)			
		ADP	ADP + MT	AMPPNP + MT	NN(+apyrase)+MT
V62C	Fast	1.50 (36%)[a]	1.52 (20%)	1.45 (22%)	1.46 (20%)
	Slow	19.4 (64%)	35.3 (80%)	28.1 (78%)	29.1 (80%)
S66C	Fast	1.48 (38%)	1.47 (20%)	1.46 (21%)	1.45(19%)
	Slow	16.6 (67%)	42.1 (80%)	38.5 (79%)	34.0 (81%)
A67C	Fast	1.43 (49%)	1.47 (29%)	1.46 (31%)	1.47 (31%)
	Slow	18.1 (51%)	19.1 (71%)	21.2 (69%)	31.4 (69%)
M68C	Fast	1.42 (44%)	1.46(24%)	1.46 (19%)	1.48 (15%)
	Slow	10.9 (56%)	12.3 (76%)	15.0 (81%)	16.4 (85%)
I70C	Fast	1.45 (36%)	1.46 (17%)	1.47 (17%)	1.48(15%)
	Slow	23.7 (64%)	40.6 (83%)	41.8 (83%)	36.8 (85%)
K72C	Fast	–	1.48 (39%)	1.51 (40%)	1.49 (36%)
	Slow	–	27.4 (61%)	23.3 (60%)	39.3 (64%)
R114C	Fast	1.46 (34%)	1.50 (17%)	1.52 (21%)	1.52 (14%)
	Slow	6.41 (66%)	8.89 (83%)	10.8 (79%)	7.44 (86%)

[a] Values in parentheses are the proportions of the fast and slow components.

α-1 and α-2 helices fluctuate between long and short inter-helix distance states.

To investigate the different ATP hydrolysis intermediates of the double-labeled kinesin mutants in the presence of MTs, three nucleotide conditions were used: (i) an ADP-bound state, (ii) an AMPPNP-bound state, and (iii) an apo state in the absence of any nucleotide [no-nucleotide (NN)]. These data are shown in Fig. 3B–D, respectively. In all cases, the EPR spectra were again broadened, implying that the spin–spin distances were less than 2.5 nm. The spectrum obtained in the presence of AMPPNP is very similar to that obtained in the MT-free state. In fact, there was a population (20%) with its distribution centered at 1.43 nm with a full-width at half maximum of 0.13 nm; the remaining fraction of spins (80%) was beyond the sensitivity limit of the method (>2.5 nm). In the no-nucleotide (NN) state, the spectrum was different and much broader. There was a larger population (41%) having a somewhat narrow distribution (full-width at half maximum = 0.41 nm) centered at 1.48 nm, and the remaining population (59%) was beyond the sensitivity limit (>2.5 nm). These results indicate that a population (21%) of helices transitioned from a longer to a shorter inter-helix distance state when nucleotides were removed. It is therefore suggested that a shift of the equilibrium between the positions of the α-1 and α-2 helices occurs upon nucleotide binding and release. In the ADP-bound state, the spectrum was an intermediate between those observed in the AMPPNP-bound state and no-nucleotide (NN) state. Fitting showed a fraction (25%) with a distance distribution centered at 1.40 nm and a full-width at half maximum of 0.24 nm, and the remaining spins (75%) were beyond the sensitivity limit (>2.5 nm).

3.4. Implications of the conformational dynamics of the α-1 helix in the presence of MTs during the ATPase cycle

We have measured the mobility and distance of spin labels attached to the α-1 and α-2 helices of kinesin monomer. Inter-helix distance measurements in double-labeled, ADP-bound kinesin indicated that upon MT binding, the fraction of spins exhibiting a short inter-helix distance with a narrow distribution increased from 20% to 25%. On the other hand, the results from the single-labeled kinesins revealed that binding MTs increased the fraction of labels in the slow motional state by ~20% (thereby decreasing the fraction in the fast motional state by ~20%). The fraction of mobility change was much larger than that of distance change. Therefore, the effect of MT binding on mobility could be interpreted as inducing both (i) a transition to a state having a shorter inter-helix distance with a narrow distribution and (ii) a fast-to-slow shift in the equilibrium between side chain motional states in the conformations with longer inter-helix distances. Binding of nucleotide (ADP or AMPPNP) to kinesin in the presence of MTs increased the fraction of the fast mobility component by ~5% at the residues M68C and R114C. Inter-helix distance measurements also showed that a substantial fraction (15–20%) of the helices transition from shorter to longer inter-helix distances upon nucleotide binding. Closer examination of the effects of nucleotide binding on residue mobility and inter-helix distance (i.e., AMPPNP and ADP effects on R114C and AMPPNP effects on M68C) revealed that they are quantitatively consistent when the equilibrium constants between fast and slow components are assumed to be 0.25 and 0 for the long

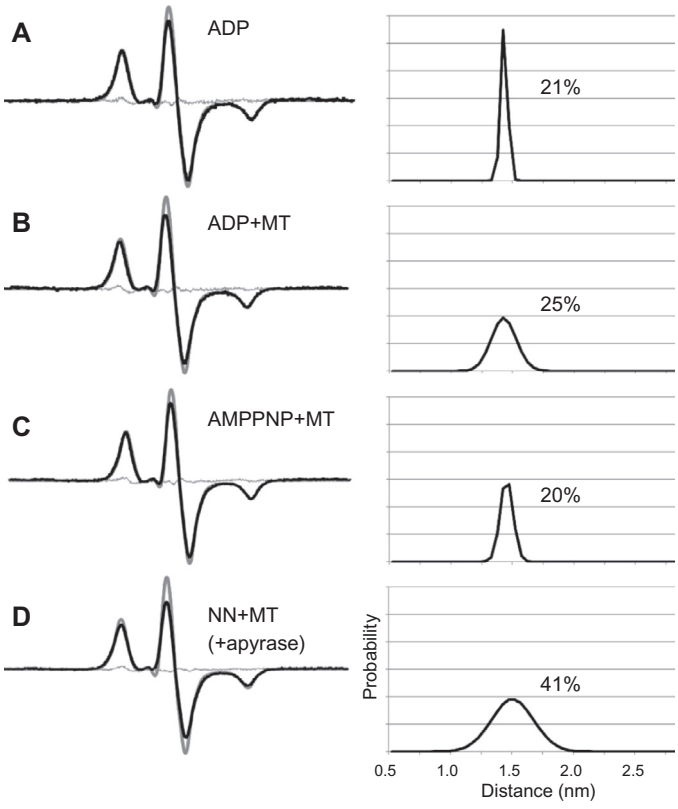

Fig. 3. Distance analysis of the EPR spectra from the double-labeled K68C/R114C kinesin mutant. The EPR spectra were obtained at 173 K under several nucleotide conditions, with or without MTs. (A) The ADP-bound state in the absence of MTs. (B) The ADP-bound state in the presence of MTs. (C) The AMPPNP-bound state in the presence of MTs. (D) The apo or no nucleotide (NN) state in the presence of MTs. The scan width is 200 G. For each state, the left panel compares the experimental spectrum of the double-labeled kinesin mutant (black line) with the spectrum of the single-labeled mutant (thick gray line) normalized to the same number of spins. The experimental spectra are fitted satisfactorily by a single Gaussian distance distribution (right panel) with some fraction of spins occurring beyond the sensitivity limit (>2.5 nm). The percentages shown are the fraction of the total spins with an inter-helix distance characterized by the single Gaussian distribution: 100 × (1 – fraction of spins > 2.5 nm apart). Residuals from the best-fit spectra (thin gray lines) are shown on the left panel.

and short distance states, respectively. However, the effect of ADP on the fraction of the fast mobility component at residue M68C appeared unexpectedly larger compared with the other residues, in which the effects of nucleotides were small or absent. It is further assumed that the equilibrium constant between the fast and slow components in the long distance state increased from 0.25 to 0.32 upon ADP binding at residue M68C, while it decreased from 0.25 to ~0.2 upon the binding of either AMPPNP or ADP at residues V62C, S66C, A67C, and I70C and from 0.6 to ~0.5 at residue K72C. Such small changes in the equilibrium constant might be produced by small changes in steric hindrance around the side-chains associated with nucleotide-induced changes in orientation, rotation, or bending of the α-1 helix in the long distance state.

In conclusion, upon nucleotide binding in the presence of MTs, the two helices move apart in a substantial fraction of kinesins as a result of a shift in the positional equilibrium. The schematic representation of MT-dependent and nucleotide-dependent conformational changes of the α-1 helix are illustrated in Fig. 4. It is an attractive possibility that upon binding of the N-terminal region of the α-1 helix to the adenine ring of ATP, the C-terminal region of the α-1 helix approaches the neck-linker (NL) and enhances the docking probability of the NL to the motor domain. It should be noted that the position of the α-1 helix in the ADP-bound state is an intermediate between those in the AMPPNP-bound state and the NN state, but it is much closer to the former than the latter. NL docking might be controlled by some other element, i.e., the structural linkage of switch II helix, switch I and P-loop to the γ-phosphate of ATP [16–20] as well as binding of the α-1 helix to the adenine ring. The present study also predict that upon MT binding in the ADP state the α-1 helix is immobilized and undergoes a small shift of its positional equilibrium away from the adenine ring

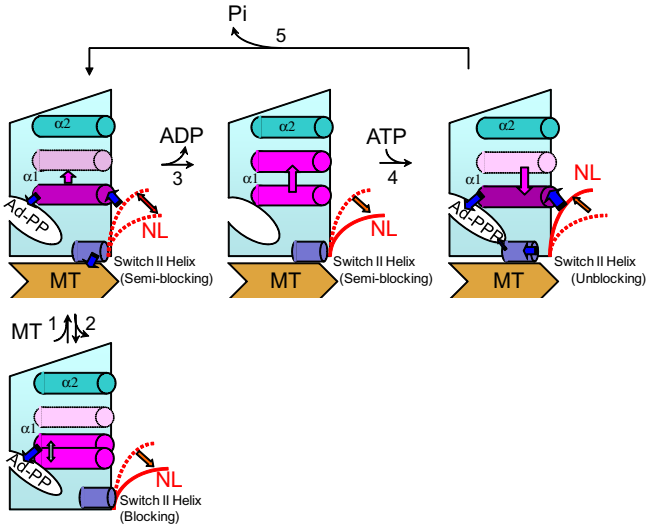

Fig. 4. Proposed conformations of the α-1 helix in the ATPase intermediate states of kinesin in the presence of MT. Protein–protein and protein-nucleotide interactions are shown as blue arrows. The equilibrium shift of the neck linker (NL) binding and α-1 helix position are represented in the red and purple arrows, respectively. *Step* 1: The binding of a MT to the motor domain, causing reduced flexibility of the backbone of the α-1 helix and partial binding of NL. *Step* 2: The unbinding of a MT from the motor domain. *Step* 3: The dissociation of adenine ring of ADP from the N-terminal end of the α-1 helix, causing a shift in the positional equilibrium of the α-1 helix such that it is closer to the α-2 helix. This shift buries the C-terminal region of the α-1 helix, resulting in unbinding of NL from the C-terminal region. *Step* 4: The binding of the adenine ring of ATP to the N-terminal end of the α-1 helix, causing a shift in the positional equilibrium of the α-1 helix away from the α-2 helix. This shift exposes the C-terminal region of the α-1 helix, resulting in rebinding of NL to the C-terminal region. *Step* 5: ATP hydrolyzes. (For interpretation of the references to color in this figure legend, the reader is referred to the web version of this article.)

of ADP to lower the affinity and promote ADP release from a catalytic site. In the apo (NN) state, the α-1 helix moves further away and the catalytic site opens fully, while in the AMPPNP or ATP state the α-1 helix again approaches the adenine ring to close the catalytic site.

3.5. Relation to other works

From chemical crosslinking experiments, Hahlen et al. [26] suggested that flexibility or structural changes in the α-1 helix is required for the ATPase activity of kinesin. High-resolution cryo-EM studies of human conventional kinesin bound to MT in the absence or presence of nucleotide were reported by Sindelar et al. [20]. This report showed that the electron density of the α-1 helix bound to AMPPNP in the presence of MTs was lower than that in the apo (NN) or ADP-bound state. This result suggests that the α-1 helix fluctuates in the AMPPNP state. This suggestion is consistent with our model, where the conformational state with a longer inter-helix distance exhibits high spin label mobility and high flexibility of the peptide side-chain and backbone. The fraction of kinesins with the longer inter-helix distance was larger in the AMPPNP-bound state than those in either the ADP-bound state or in the apo (NN) state in the presence of MTs. The spin label mobility in the AMPPNP state was also higher than that in the apo state, although it was almost indistinguishable (within error) from the ADP-bound state.

Cryo-EM study [20] also showed that the nucleotide binding pocket opens in the ADP state on MTs and fully in the apo state by displacement of the α-1 helix as well as switch I loop, as compared with that in the AMPPNP state on MTs. This view is consistent with our finding of the α-1 helix movement at the active catalytic site, displacing away from the adenine ring upon MT binding in the ADP state, further away in the apo state on MTs and approaching the ring in the AMPPNP state (See Fig. 4). More information from spin labels attached at the other residues will be required to establish detailed structural changes within the kinesin motor domain at high resolution for comparison with the other structural studies.

3.6. Conclusions

In this study, we used site-directed spin labeling EPR to directly detect the key structural change within the kinesin catalytic domain that defines the NL power stroke as well as the nucleotide-induced displacement and dynamics of the α-1 helix. Our results show that the α-1 helix changes its positional state upon ADP release and ATP binding. These results provide direct insight into one of the most important aspects of kinesin enzymology, the coordination of MT-activated ADP release and ATP binding and the power stroke of the kinesin NL.

Acknowledgments

This research was supported by Grants-in-Aid from the Special Coordination Funds, the Scientific Research on Priority Areas from the Ministry of Education, Culture, Sports, Science and Technology, and the Core Research for Evolutional Science and Technology program from the Japanese Science and Technology Cooperation, Japan.

Appendix A. Supplementary data

Supplementary data associated with this article can be found, in the online version, at http://dx.doi.org/10.1016/j.bbrc.2013.12.063.

References

[1] S.T. Brady, A novel brain ATPase with properties expected for the fast axonal transport motor, Nature 317 (1985) 73–75.
[2] R.D. Vale, B.J. Schnapp, T.S. Reese, M.P. Sheetz, Movement of organelles along filaments dissociated from the axoplasm of the squid giant axon, Cell 40 (1985) 449–454.
[3] N. Hirokawa, Y. Noda, Y. Okada, Kinesin and dynein superfamily proteins in organelle transport and cell division, Curr. Opin. Cell Biol. 10 (1998) 60–73.
[4] M. Tomishige, R.D. Vale, Controlling kinesin by reversible disulfide cross-linking: Identifying the motility-producing conformational change, J. Cell Biol. 151 (2000) 1081–1092.
[5] S. Rice, A.W. Lin, D. Safer, C.L. Hart, N. Naber, B.O. Carragher, S.M. Cain, E. Pechatnikova, E.M. Wilson-Kubalek, M. Whittaker, E. Pate, R. Cooke, E.W. Taylor, R.A. Milligan, R.D. Vale, A structural change in the kinesin motor protein that drives motility, Nature 402 (1999) 778–784.
[6] C.V. Sindelar, M.J. Budny, S. Rice, N. Naber, R. Fletterick, R. Cooke, Two conformations in the human kinesin power stroke defined by X-ray crystallography and EPR spectroscopy, Nat. Struct. Biol. 9 (2002) 844–848.
[7] S. Rice, Y. Cui, C. Sindelar, N. Naber, M. Matuska, R.D. Vale, R. Cooke, Thermodynamic properties of the kinesin neck-region docking to the catalyic core, Biophys. J. 84 (2003) 1844–1854.
[8] R. Nitta, Y. Okada, N. Hirokawa, Structural model for strain-dependent microtubule activation of Mg-ADP release from kinesin, Nat. Struct. Mol. Biol. 15 (2008) 1067–1075.
[9] W.L. Hubbell, A. Gross, R. Langen, M.A. Lietzow, Recent advances in site-directed spin labeling of protein, Curr. Opin. Struct. Biol. 8 (1998) 649–656.
[10] W.L. Hubbell, D.S. Cafiso, C. Altenbach, Identifying conformational change with site-directed spin labeling, Nat. Struct. Biol. 7 (2000) 735–739.
[11] M.D. Rabenstein, Y.K. Shin, Determination of the distance between two spin labels attached to a micromolecule, Proc. Natl. Acad. Sci. USA 92 (1995) 8239–8243.
[12] K. Sugata, M. Nakamura, S. Ueki, P.G. Fajer, T. Arata, ESR reveals the mobility of the neck linker in dimeric kinesin, Biochem. Biophys. Res. Commun. 314 (2004) 447–451.
[13] M.D. Yamada, S. Maruta, S. Yasuda, K. Kondo, H. Maeda, T. Arata, Conformational dynamics of loops L11 and L12 of kinesin as revealed by spin-labeling EPR, Biochem. Biophys. Res. Commun. 364 (2007) 620–626.
[14] K. Sugata, L. Song, M. Nakamura, S. Ueki, P.G. Fajer, T. Arata, Nucleotide-induced flexibility change in neck linkers of dimeric kinesin as detected by distance measurements using spin-labeling EPR, J. Mol. Biol. 386 (2009) 626–636.
[15] N. Naber, S. Rice, M. Matuska, R.D. Vale, R. Cooke, E. Pate, EPR spectroscopy shows a microtubule-dependent conformational change in the kinesin switch 1 domain, Biophys. J. 84 (2003) 3190–3196.
[16] R.D. Vale, Switches, latches, and amplifiers: common themes of G proteins and molecular motors, J. Cell Biol. 135 (1996) 291–302.
[17] M. Kikkawa, E.P. Sablin, Y. Okada, H. Yajima, R.J. Fletterick, N. Hirokawa, Switch-based mechanism of kinesin motors, Nature 411 (2001) 439–445.
[18] K. Hirose, E. Akimaru, T. Akiba, S.A. Endow, L.A. Amos, Large conformational changes in a kinesin motor catalyzed by interaction with microtubules, Mol. Cell 23 (2006) 913–923.
[19] C.V. Sindelar, K.H. Downing, The beginning of kinesin's force-generating cycle visualized at 9 Å resolution, J. Cell Biol. 177 (2007) 377–385.
[20] C.V. Sindelar, K.H. Downing, An atomic-level mechanism for activation of the kinesin molecular motors, Proc. Natl. Acad. Sci. USA 107 (2010) 4111–4116.
[21] S. Sack, J. Müller, A. Marx, M. Thormählen, E.M. Mandelkow, S.T. Brady, E. Mandelkow, X-ray structure of motor and neck domains from rat brain kinesin, Biochemistry 36 (1997) 16155–16165.
[22] D.D. Hackney, Kinesin ATPase: rate-limiting ADP release, Proc. Natl. Acad. Sci. USA 85 (1988) 6314–6318.
[23] M.D. Yamada, Y. Nakajima, H. Maeda, S. Maruta, Photocontrol of kinesin ATPase activity using an azobenzene derivative, J. Biochem. 142 (2007) 691–698.
[24] S. Ueki, M. Nakamura, T. Komori, T. Arata, Site-directed spin labeling electron paramagnetic resonance study of the calcium-induced structural transition in the N-domain of human cardiac troponin C complexed with troponin I, Biochemistry 44 (2005) 411–416.
[25] P. Fajer, L. Song, Practical pulsed dipolar EPR (DEER), in: M. Hemminga, L. Berliner (Eds.), Biological Magnetic Resonance, vol. 27, Springer, New York, 2007, pp. 95–128.
[26] K. Hahlen, B. Ebbing, J. Reinders, J. Mergler, A. Sickmann, G. Woehlke, Feedback of the kinesin-1 neck-linker position on the catalytic site, J. Biol. Chem. 281 (2006) 18868–18877.